Formation of Multiscale Porous Surfaces via Evaporation-Induced Aggregation of Imprinted Nanowires with Highly Viscous Photocurable Materials

Myung Seo Kim , Seungwoo Shin , Woo Young Kim , Sang Hoon Lee , Seo Rim Park , Seok Kim * , Young Tae Cho *

Posted Date: 3 January 2024

doi: 10.20944/preprints202401.0278.v1

Keywords: Anodic Aluminum Oxide(AAO); Nano-wires; UV Curable Resin; Viscosity; Surface Tension; High Aspect Ratio; Surface Treatment

Article

Formation of Multiscale Porous Surfaces via Evaporation-Induced Aggregation of Imprinted Nanowires with Highly Viscous Photocurable Materials

Myung Seo Kim [1], Seungwoo Shin [1], Woo Young Kim [1], Sang Hoon Lee [1], Seo Rim Park [1], Seok Kim [2,*] and Young Tae Cho [2,*]

[1] Department of Smart Manufacturing Engineering, Changwon National University (CWNU), South Korea.; 20215000@gs.cwnu.ac.kr

[2] Department of Mechanical Engineering, Changwon National University (CWNU), South Korea ; kimseok@changwon.ac.kr ; ytcho@changwon.ac.kr

* Correspondence: ytcho@changwon.ac.kr; Tel.: +82-55-213-3608

Abstract: Numerous structures at the nano- and microscale manifest distinctive properties with far-reaching implications across diverse fields, including electronics, electricity, medicine, and surface engineering. Established methods such as nanoimprint lithography, photolithography, and self-assembly play crucial roles in the fabrication of nano- and microstructures; however, they exhibit limitations in generating high-aspect-ratio structures when utilizing high-viscosity photocurable resins. In response to this inherent challenge, we propose a highly cost-effective approach facilitating the direct replication of high-aspect-ratio structures, specifically nanowires, through the utilization of anodized aluminum substrates. This study elucidates the streamlined fabrication process for multiscale porous surfaces achieved through the evaporation-induced integration of solid nanowires printed with high-viscosity photocurable resin.

Keywords: Anodic Aluminum Oxide(AAO); Nano-wires; UV Curable Resin; Viscosity; Surface Tension; High Aspect Ratio; Surface Treatment

1. Introduction

Nanoscale structures play a pivotal role in various fields, such as fuel cells [1,2], biomaterial surfaces [3,4], electronics [5], and electrical engineering [6], establishing them as highly regarded technology. These structures are crafted using methods such as lithography [7], sol-gel [8], self-assembly [9,10], direct replication using Anodic Aluminum Oxide (AAO) [11–14], and SPPW [15–17]. Nanoimprint lithography (NIL) [18–22], a technology employing roll imprinting to create nanopatterns by coating a resin that cures with ultraviolet light, is particularly esteemed for its simplicity and cost-effectiveness. However, the nature of NIL, involving the transfer of thin layered materials through pressure to create patterns on a new surface, imposes limitations on achieving structures with high aspect ratios.

An efficient method known for fabricating nanoscale high-aspect-ratio structures, such as nanowires, involves the use of AAO substrates, known for their ease of use and cost-effectiveness [23,24]. AAO substrates possess numerous nanoscale pores and microscale heights, facilitating the fabrication of uniform, high-aspect-ratio nanowires. Despite these advantages, studies on AAO have revealed that AAO-based nanowires tend to aggregate when the aspect ratio exceeds 15:1 due to the surface tension of the etchant during wet etching of the AAO substrate used as a mold. This observation highlights the potential for creating nano-micro multiscale structures [25,26].

In this study, we endeavored to create a nano-micro multiscale structure with a high aspect ratio by harnessing the aggregation phenomenon of nanowires caused by surface tension during wet etching. Experimental results demonstrated a strong correlation between surface aggregation,

 doi:10.20944/preprints202401.0278.v1

nanowire length, and the viscosity of the resin. Filling the substrate pores with photocurable resin to create nanowires presented challenges due to the nature of the AAO substrate, which features nanometer-sized pores. Consequently, the roll pressing process was employed as a method to fill the AAO substrate. When pressurized through a roll, the photocurable resin ascends along the microscopic pores of the AAO substrate due to the applied force. The rising height is assumed to be consistent, as it is proportional to the pressing force. UV light-curable resins with three different viscosities (8.51 cPs, 307.92 cPs, 2588.55 cPs) were used in this study. These resins were placed between PET (polyethylene terephthalate) and AAO substrates and filled the pores of the AAO substrate through roll pressing. Each resin rose due to pressure, filling the pores of the AAO substrate to the end, and the higher the viscosity of the resin, the greater the force required to maintain the raised height, resulting in longer nanowires.

The height of the generated nanowire is closely linked to the ability to sustain the increased resin height, with surface tension and capillary force exerting significant influence. In the capillaries constituting the AAO, liquid resin moves through a flow in a microscopic space as it descends. For high-viscosity resin, the interaction of the molecules making up the liquid resin acts strongly at the three-phase interface formed by the wall of air-resin-AAO. Due to this intense interaction at the interface, the resin flows along the wall of the AAO substrate pore, preventing it from descending. Consequently, nanowires produced using high-viscosity resin appear longer than those produced with low-viscosity resin.

A wet etching process using NaOH solution was employed to separate the resulting nanowires from the substrate, and the resulting structural properties were analyzed based on nanowire viscosity. The resulting surface exhibited porous features with smaller and denser pores, demonstrating that the height of nano-micro multiscale structures can be controlled through viscosity differences. This study underscores the viscosity of resin as a critical factor in nanowire production. Additionally, the surface of the generated structure was crafted as an array of micro-sized structures [27], with the anticipated advantage of increasing surface hydrophobicity [28–30]. Consequently, surface treatment (UV-O: Ultraviolet ozone [31–35], OTS: Octadecyl-trichlorosilane [36–38]), a simple method to enhance surface properties, was conducted. The degree of improvement in surface properties was measured by determining the contact angle [39] after each treatment and simultaneous treatment, and the impact of surface treatment on the enhancement of surface properties was analyzed.

2. Fabrication of Nano-Wires

2.1. Method for Producing Nano-Wires using AAO as a Substrate

In this study, nanowires were fabricated through direct replication using AAO substrates (Whatman, anodisc 25, pore diameter 200 nm, thickness 60 μm). Figure 1 provides an overview of the nanowire creation process. After cleaning the PET substrate with isopropyl alcohol (IPA), 1 ml of UV-curable resin was dispensed onto the PET. AAO substrates were then placed on each of the three UV-curable resins selected based on their dispensed viscosity. At this stage, the UV-curable resin slowly spread out, filling many pores of the AAO substrate. Notably, it was observed that low-viscosity photocurable resin and medium-viscosity photocurable resin, having relatively low viscosity, self-filled the AAO substrate more rapidly than high-viscosity photocurable PDMS. However, due to the high viscosity of high-viscosity photocurable PDMS, it required more time to self-fill the very small pores of the AAO substrate. To address this, rollers were used to sequentially apply pressure to all three resins, allowing them to rise through the various pores of the AAO substrate through optical action. All three resins were pressurized to maintain consistent experimental conditions.

Preprints (www.preprints.org) | NOT PEER-REVIEWED | Posted: 3 January 2024 doi:10.20944/preprints202401.0278.v1

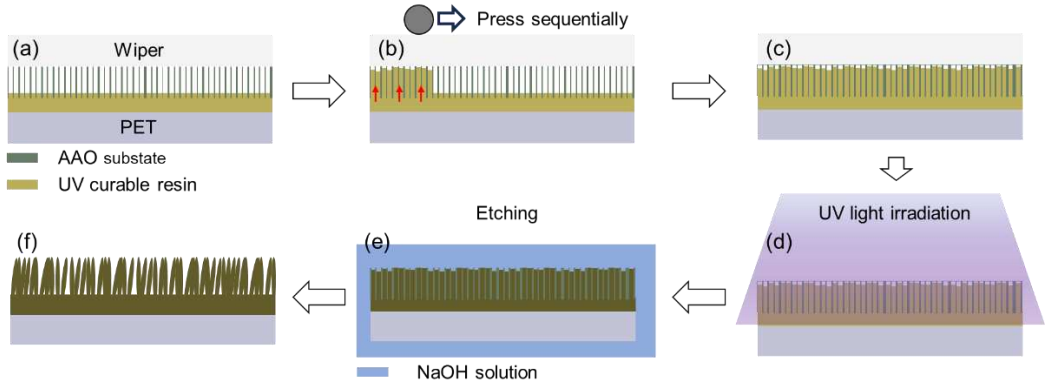

Figure 1. Schematic diagram of fabrication nanowire process.

Subsequently, the resin was cured using an LED curing device for the appropriate duration (low-viscosity photocurable resin: 4 sec / 440 mJ/cm², medium-viscosity photocurable resin: 2 sec / 220 mJ/cm², high-viscosity photocurable PDMS: 70 sec / 7,700 mJ/cm²). The AAO substrate, with a pore size of 200 nm and a thickness of 60 μm, exhibited a high aspect ratio of 120:1, resulting in nanowires with a similarly high aspect ratio structure. These nanowires filled the various pores of the AAO substrate, ensuring intrinsic adhesion between the substrate and the resulting nanowires. Given the vulnerability of AAO substrates to external forces, even slight forces could cause serious damage, rendering physical removal of the substrate impossible. Numerous studies using AAO have demonstrated that AAO substrates can be removed using various etching solutions (NaOH, KOH). Etching experiments were conducted with a 2 molar NaOH etchant during the same etching period. The NaOH solution exhibited the highest etching efficiency and could penetrate even the smallest nano-sized pores. Scanning electron microscope (SEM) observations confirmed the etching efficiency, showcasing the creation of nanowires aggregated to form numerous pores.

To separate the cured nanowires from the AAO substrate, the substrate was etched in a 2 molar NaOH solution for 10 min. Subsequently, it was washed with DI water, and the surface was dried with a blower. Figure 3 illustrates a scenario where the etched nanowires do not stand straight and aggregate. These nanowires were formed by filling various pores of the AAO substrate after curing with ultraviolet light. However, owing to the nature of high-aspect-ratio nanowires, they separated from the substrate during etching and densely aggregated due to surface tension, forming a nonlinear array. This phenomenon is influenced by viscosity and manifests differently depending on the viscosity.

Figure 2. The rise of resin due to pressurization.

Preprints (www.preprints.org) | NOT PEER-REVIEWED | Posted: 3 January 2024 doi:10.20944/preprints202401.0278.v1

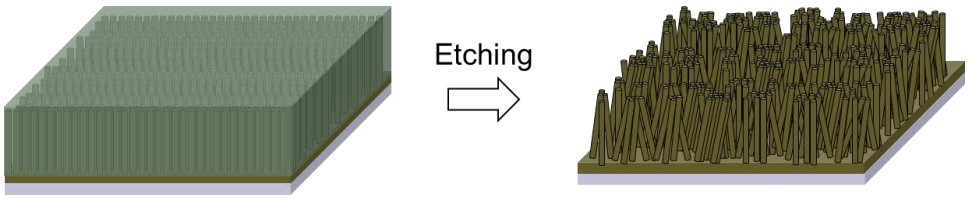

Figure 3. When removing the nanowires from the AAO substrate through etching, the nanowires do not stand in a straight line due to surface tension and aggregate.

2.2. Height of Nano-Wires According to Resin Viscosity

In this study, nanowires were fabricated using low-viscosity photocurable resin, medium-viscosity photocurable resin, and high-viscosity photocurable PDMS with varying viscosities. During the subsequent etching process, nano-micro multi-scale structures were created through surface tension acting on the nanowires. Previous studies on nanowire fabrication using AAO substrates have revealed that the viscosity of the resin significantly impacts the length of the nanowires and the pore size created by agglomeration in the formation of nano-micro multiscale structures. Higher viscosity results in longer nanowires and smaller pore sizes.

To isolate the effect of viscosity, the fabrication process followed previous research methods. Subsequently, the resulting nanowires after etching and blow-drying were analyzed using SEM equipment. Upward-viewing images were used to measure the pore size, and side-viewing images were used to measure the height of the nanowires that constitute the nano-micro multiscale structures. Figure 4 presents top and side-view SEM images of nanowires fabricated using the three resins. Height measurement of the nanowires involved collecting heights from a total of 10 locations and calculating the average. The results were as follows: low viscosity photocurable resin: 35.21 ± 3.08 μm, medium viscosity photocurable resin: 46.72 ± 4.90 μm, high viscosity photocurable PDMS: 51.82 ± 2.11 μm.

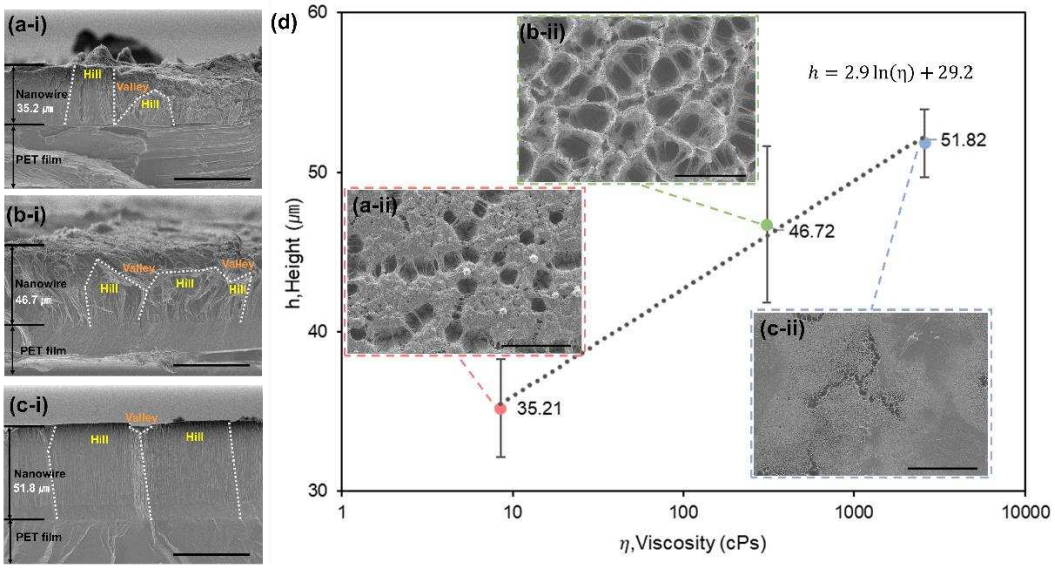

Figure 4. SEM image of nanowires fabricated through UV curable resin. low viscous photocurable resin, medium viscous photocurable resin, and high viscous photocurable PDMS (**a**) Low viscous photocurable resin; (**b**) Medium viscous photocurable resin; (**c**) High viscous photocurable PDMS; (**i**) Top view of nanowires (x1000); (**ii**) Side view of nanowires (x1000); All scale bars are 50 μm.

Medium viscosity photocurable resins with denser pores revealed that pore formation led to the creation of valleys, resulting in greater height variations. On the other hand, high-viscosity photocurable PDMS with the smallest and densest pores showed the smallest height deviation. This confirms previous findings that high viscosity leads to longer nanowires. The resulting nanowires

 doi:10.20944/preprints202401.0278.v1

exhibited a relatively uniform length over the entire area, with higher viscosity filling the AAO substrate more effectively and thus resulting in longer nanowires.

The degree of twisting of the nanowires was also significantly affected by the viscosity of the resin. When observing the side surfaces of nanowires produced with low-viscosity photocurable resin, the wires appeared to entangle, causing surface formation and resulting in surface morphology. However, when using high-viscosity photocurable PDMS, which had the highest viscosity, the nanowires were nearly straight, close-packed, untwisted, and exhibited minimal twisting. This observation suggests that with lower viscosity resins, the resin cannot completely fill the AAO substrate during etching, creating more space for the etchant to penetrate the pores of the AAO substrate, causing the AAO substrate to etch more rapidly and over the entire area of the nanowires. This is due to its quick susceptibility to surface tension.

2.3. Surface of Nano-Wires According to Resin Viscosity

In this study, discernible viscosity differences were observed among the low-viscosity photocurable resin, medium-viscosity photocurable resin, and high-viscosity photocurable resin, leading to distinct variations in surface quality. Figure 4a illustrates the surface of a nano-micro multiscale structure fabricated using the lowest viscosity resin. When employing the lowest viscosity resin, the surface exhibited sparsely distributed pores, a characteristic attributed to the uniformity in the resulting nanowire length. Figure 4i provides a cross-section of a nano-micro multiscale structure created with the lowest viscosity resin. In sections forming hills, longer nanowires compared to surrounding ones were concentrated, resulting in clustered valleys toward the long nanowires, shaping the hill and creating an empty space at the top. A bridge-like structure connecting hills was also formed based on the same principle, dividing the valley and forming a pore.

Figure 4b presents a top view of the nano-micro multiscale structure produced using medium viscosity resin. Similar results were obtained with medium viscosity resin, but the pores at the top appeared larger. This can be explained by the longer nanowires in medium viscosity resins, making the high aspect ratio structure more susceptible to surface tension during wet etching. Consequently, the nanowires forming the structure did not stand straight due to the influence of surface tension, resulting in a lower structure height and larger pores compared to the created length.

Figure 4c showcases the surface of the nano-micro multiscale structure fabricated with the highest viscosity resin. In contrast to the previous two cases, the pores appeared very small, and the interval between pore creations was larger. This observation directly correlates with the viscosity of the resin used. Higher viscosity resins produce relatively high nanowires compared to low-viscosity resins, reducing the time for the etching solution to contact the entire area during wet etching. This reduction in time affected by surface tension leads to a decrease in the tendency of nanowires with a high aspect ratio to aggregate. When high-viscosity resin was used, the time under the influence of surface tension was reduced, resulting in relatively straight nanowires. Therefore, the height of the nano-micro multiscale structure was elevated, and as seen in the cross-section in Figure 4f, a relatively straight bundle of nanowires was created, with the valley appearing lower than in the previous two cases.

We quantified the degree of aggregation by measuring the size of the pores created on the surface, utilizing SEM (scanning electron microscope) equipment and data from 5 points for each specimen. Figure 4d illustrates the resulting structure height depending on the viscosity of the resin used. The graph was expressed using a logarithmic scale, and data fitting allowed the expression of the height according to the viscosity of the resin as a formula for predicting the height of the structure based on viscosity. In terms of area, measurements were 183.33 μm^2, 467.49 μm^2, and 4.42 μm^2 in that order, starting from when low-viscosity resin was used.

In summary, the length of the nanowires produced was influenced by viscosity, with higher viscosity resulting in longer nanowires. The resulting nanowires aggregated to form a surface, showing different tendencies depending on the time influenced by surface tension during wet etching. Longer times under the influence of surface tension led to the clustering of nanowires around the longer ones, forming pores. The densest pore size was found when the resin with the highest

Preprints (www.preprints.org) | NOT PEER-REVIEWED | Posted: 3 January 2024 doi:10.20944/preprints202401.0278.v1

viscosity was used, as the entire nanowire was least affected by surface tension. Consequently, we achieved the creation of nanowires with varying heights by controlling the viscosity of the resin, successfully producing a nano-micro multiscale porous structure with different pore sizes using surface tension.

3. Effect of Surface Treatment

3.1. Change in Nano-Wire Structure According to Surface Treatment

The surface of the nano-micro multiscale structure, formed through the aggregation of nanowires, displays numerous holes with a randomly arranged pattern, lacking regularity. The pore-induced surface resembles a micro-sized pattern, and existing studies have underscored the importance of these micro-sized patterns in enhancing surface properties by improving the contact angle. As evident in the cross-sectional structure of the nano-micro multiscale structure produced in this study, the repeated hills and valleys are presumed to enhance the contact angle by creating air pockets in the valley area when the liquid contacts the surface. Therefore, well-known hydrophilic UV-O treatment [29–33] and hydrophobic OTS treatment [34–36] were conducted to improve the surface properties. Among the nanowires, those fabricated using high-viscosity photocurable PDMS exhibited surfaces with particularly dense and small pores, making structures manufactured with high-viscosity resin optimal for demonstrating the effects of surface treatment.

Each treatment lasted for 60 minutes, and a total of four different surfaces were analyzed, including an untreated surface, a UV-O 60-minute treated surface, an OTS 60-minute treated surface, and a sequential treatment with UV-O for 60 minutes followed by OTS for 60 minutes.

Figure 5a displays SEM images of the nanowires from top and side views after 60 minutes of UV-O treatment. Significant changes were observed on the surface after UV-O treatment, including an expanded pore size compared to the untreated surface, with an average pore diameter of 15.5 μm. The original pore structure was disrupted, forming connections between neighboring pores. Due to the UV-O treatment, the smoothing effect of the nanowire surface is especially evident on the side surfaces. The original untreated nanowires had a straight lower part and an agglomerated upper part, with the agglomerated upper part having a relatively sharp appearance. However, after UV-O treatment, the smoothing effect due to high-energy exposure is clearly visible in the upper part, which becomes more uniform and smooth.

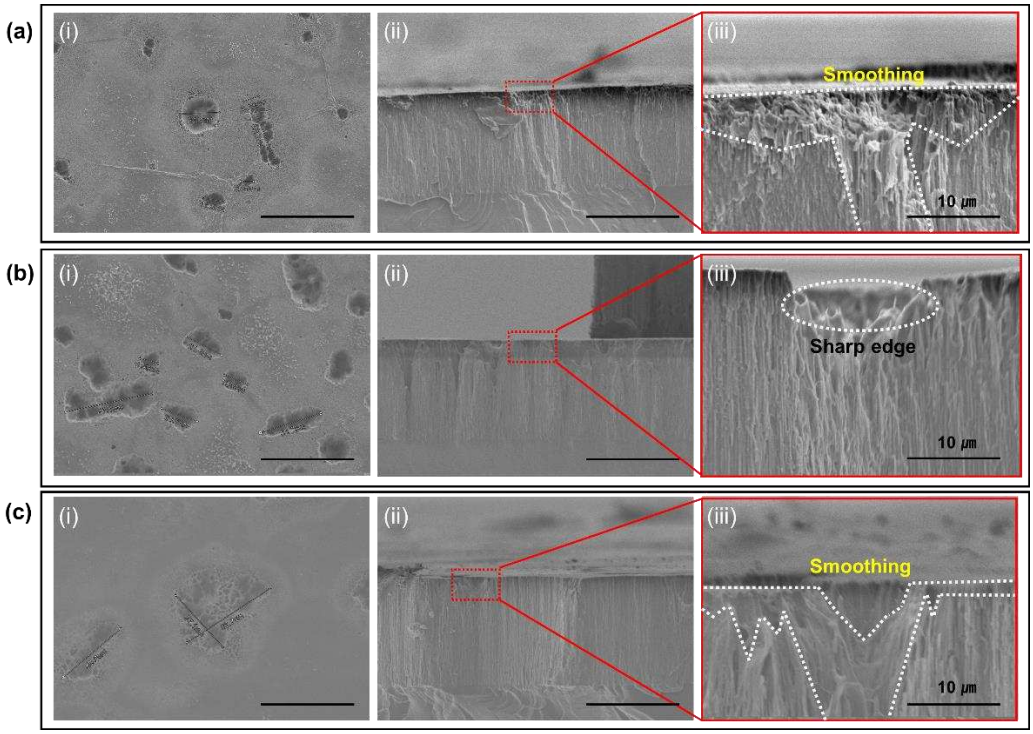

Figure 5. Changes in OTS surface after UV-O, OTS, and UV-O treatment measured via SEM (**a**) UV-O treatment for 60 min; (**b**) OTS treatment 60 min;

 doi:10.20944/preprints202401.0278.v1

(**c**) UV-O treatment for 60 min followed by OTS treatment for 60 min; (**i**) Top view (x1000); (**ii**) Side view (x1000); (**iii**) Side view (x5000). Scale bars are 50 μm except 10 μm bars.

Figure 5b shows the SEM image of the nanowires after 60 minutes of OTS treatment, capturing both top and side views. OTS treatment, performed in a vacuum box, involves uniformly dispersing the OTS solution on the nanowire surface and subjecting it to a vapor deposition process at 100 degrees Celsius for 60 minutes. OTS treatment mainly focuses on controlling water repellency and does not cause significant structural changes. Therefore, the nanowire surface showed no notable changes compared to the untreated surface, resulting in the exposed surface of the nanowire having a sharp appearance. Direct high-energy exposure to the nanowires, such as UV-O treatment, is required to induce large structural changes. However, OTS treatment simply coats silane single molecules on the nanowire surface and does not involve direct high-energy irradiation of the surface.

Figure 5c presents the SEM image of the nanowires after sequential UV-O 60-minute treatment followed by OTS 60-minute treatment. After UV-O treatment, the nanowire surface was smoothed by direct exposure to high energy. Subsequent OTS treatment did not significantly change the surface compared to surfaces subjected to UV-O treatment alone.

3.2. Changes in Wettability of Nano-Wire Surfaces According to Surface Treatment

The contact angle [37] was measured to observe changes in lamination behavior after surface treatment. A 5 μl DI aqueous solution was used for the measurement, and the experiment was conducted in a class-1000 cleanroom controlled at 45 ± 5% humidity and 21 ± 1 °C temperature. For each case, measurements were repeated five times. Initially, we measured the contact angle of the untreated nanowires and found an average of 103.9°. This is attributed to the air pockets formed at the bottom of the nanowire porous structure due to aggregation during surface formation, influencing the interaction between the DI aqueous solution and the surface.

Figure 6 illustrates the contact angle measured after dispensing 5 μl of DI water on the surface of nanowires fabricated using high-viscosity photocurable PDMS. Contact angles were determined on a total of four surfaces: the untreated surface, the surface after 60 minutes of UV-O treatment, the surface after 60 minutes of OTS treatment, and the surface after sequential treatment with 60 minutes of UV-O followed by 60 minutes of OTS. After 60 minutes of UV-O treatment, the contact angle significantly decreased to 46.3° compared to the untreated nanowire surface. This reduction is caused by increased interaction between the surface and water due to the deposition of oxygen substrate during UV-O treatment. Simultaneously, the surface of the nano-micro multiscale structure is influenced by the energy irradiated during UV-O treatment, changing smoothly and losing surface characteristics such as fine patterns.

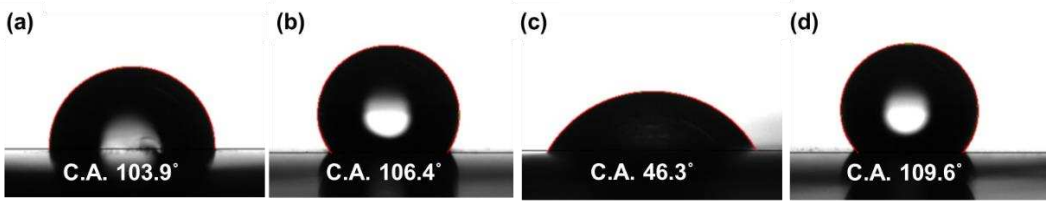

Figure 6. Measurement of contact angle of nanowires made of high viscous photocurable PDMS after dispensing 5ul of DI water (**a**) Contact angle of untreated surface; (**b**) Contact angle of nanowire surface after 60 minutes of UV-O treatment; (**c**) After 60 minutes of OTS treatment Contact angle of the nanowire surface; (**d**) Contact angle of the nanowire surface treated with UV - O and OTS sequentially for 60 minutes each.

In contrast, after 60 minutes of OTS treatment, the contact angle of the nanowires increased to 106.04° compared to the untreated surface. This increase is attributed to the bonding of OTS with the oxygen substrate on the surface, resulting in hydrophobic properties due to OTS treatment. The

 doi:10.20944/preprints202401.0278.v1

contact angle did not increase significantly because the effect of the air pocket at the bottom was dominant over the effect of OTS treatment as a factor representing the hydrophobic nature.

The contact angle of the surface treated with UV-O for 60 minutes and then treated with OTS for 60 minutes was measured to be 109.6°, which is similar to the result of OTS treatment alone. The hydrophobic performance of the OTS solution was enhanced during the gas deposition process because the oxygen substrate bound to the surface significantly increased due to the enhanced interaction during UV-O treatment. This effect is more evident on surfaces with combined UV-O and OTS treatments, showing contact angles similar to those with OTS treatment alone.

3. Conclusions

In this study, we fabricated nanowires using three types of resins: low-viscosity photocurable resin (8.51 cPs), medium-viscosity photocurable resin (307.92 cPs), and high-viscosity photocurable PDMS (2588.55 cPs), followed by inducing surface aggregation. We propose a simple and efficient method for fabricating nano-micro multi-scale structures. Structural changes in nano-micro multi-scale structures due to variations in viscosity were clearly demonstrated. Using a roll, we filled nanometer-sized pores with nanometer diameter and microheight, and AAO pores with micrometer height with photocurable resin through pressure. Subsequently, a UV light source was irradiated through an LED curing machine, and after etching, nano-micro multi-scale structures with different heights and surface shapes were created depending on the viscosity difference.

The difference in height of the generated structure was attributed to the viscosity of the photocurable resin used, confirming that higher viscosity resulted in nanowires forming the structure closer to a straight line. Particularly, by employing high-viscosity photocurable PDMS with relatively high viscosity, we successfully created a taller structure than in previous studies, emphasizing the significant effect of resin viscosity on the length of the nanowires forming the structure.

The structure produced through curing after UV light irradiation was strongly bonded to AAO, making physical demolding impossible. To address this issue, etching was performed using a NaOH solution. During the etching process, as the AAO substrate disappeared, the high aspect ratio nanowires were unable to stand in a straight line due to surface tension, appearing to aggregate. The surface of the structure created in this process exhibited a porous surface. The porous structure's characteristics were also influenced by the resin viscosity, with high-viscosity photocurable PDMS resulting in a relatively dense and fine porous structure.

The height of the structure, measured by the generated nanowire using SEM, was as follows: low-viscosity photocurable resin: 35.21 ± 3.08 μm, medium-viscosity photocurable resin: 46.72 ± 4.90 μm, and high-viscosity photocurable PDMS: 51.82 ± 2.11 μm. The structure created with low-viscosity photocurable resin had the lowest height, while the one made with high-viscosity photocurable PDMS exhibited the highest height. This is attributed to the stronger force maintaining the position when filling the AAO substrate with higher viscosity resin through roll pressure, and the extended duration when demolding the AAO substrate through etching.

Regarding surface properties, all three cases produced surfaces with porous structures. High-viscosity photocurable PDMS, in particular, resulted in surfaces with very small pores, averaging 4.42 μm^2. Surfaces created with high-viscosity photocurable PDMS exhibited dense and porous characteristics, resembling hydrophobic properties similar to superhydrophobic surfaces.

UV-O zone and OTS treatments were conducted to investigate structural changes and contact angles of the nanowires. UV-O zone treatment smoothed the surface, creating new pore structures, and the deposition of high oxygen substrates made the surface hydrophilic. In contrast, OTS treatment primarily affected the contact angle without causing significant structural changes, imparting hydrophobicity to the nanowire surface and increasing the contact angle. When UV-O zone and OTS treatments were performed sequentially, the surface became smooth, similar to UV-O zone treatment alone, but the contact angle was further improved due to the hydrophobic effect caused by OTS treatment. However, since the structural changes induced by UV-O zone treatment played a major role, the increase in the measured contact angle was minimal. This demonstrates the potential to control the structural and contact angle properties of nanowires through simple surface treatments.

In conclusion, this study presented an efficient method to create a nano-micro multi-scale porous structure made of nanowires using an AAO substrate. The investigation examined the effect of resin viscosity on the height and surface formation of the structure. Using high-viscosity photocurable PDMS allowed the creation of a taller structure, highlighting the significance of viscosity as a crucial factor affecting the height of the structure. The results of this study offer valuable insights into strategies for creating effective nano-micro multiscale porous structures for nanotechnology applications, suggesting a range of possibilities. Additionally, the study provides fundamental insights into the correlation between resin viscosity, nano-micro structure height, and porous surface formation, offering useful information for selecting resins with desired surface properties.

Acknowledgments: This work has supported by the Korea Institute of Machinery & Materials, Republic of Korea, under the project name of "Development of self-aligned microlens array for improvement patterning resolution in DMD-based digital lithography"(Project ID : NK242E) and This work was supported by "Regional Innovation Strategy (RIS)" through the National Research Foundation of Korea(NRF) funded by the Ministry of Education(MOE)(2021RIS-003).

Conflicts of Interest: The authors declare no conflict of interest.

References

1. Pandiyan, G. Karthik, and T. Prabaharan. "Implementation of nanotechnology in fuel cells." Materials Today: Proceedings 33 (2020): 2681-2685. https://doi.org/10.1016/j.matpr.2020.01.368
2. Ghasemi, Mostafa, et al. "Nano-structured carbon as electrode material in microbial fuel cells: A comprehensive review." Journal of Alloys and Compounds 580 (2013): 245-255. https://doi.org/10.1016/j.jallcom.2013.05.094
3. Sarikaya, Mehmet, et al. "Molecular biomimetics: nanotechnology through biology." Nature materials 2.9 (2003): 577-585. https://doi.org/10.1038/nmat964
4. Ramos, Ana P., et al. "Biomedical applications of nanotechnology." Biophysical reviews 9.2 (2017): 79-89. https://doi.org/10.1007/s12551-016-0246-2
5. Ghouse, Hiba, et al. "Importance of nanotechnology, various applications in electronic field." Nanotechnology for Electronic Applications (2022): 1-28. https://doi.org/10.1007/978-981-16-6022-1_1
6. Contreras, J. E., E. A. Rodriguez, and J. Taha-Tijerina. "Nanotechnology applications for electrical transformers—A review." Electric Power Systems Research 143 (2017): 573-584. https://doi.org/10.1016/j.epsr.2016.10.058
7. Xia, Younan, and George M. Whitesides. "Soft lithography." Annual review of materials science 28.1 (1998): 153-184. https://doi.org/10.1146/annurev.matsci.28.1.153
8. Livage, Jacques. "Sol-gel processes." Current Opinion in Solid State and Materials Science 2.2 (1997): 132-138. https://doi.org/10.1016/S1359-0286(97)80057-5
9. Whitesides, George M., and Bartosz Grzybowski. "Self-assembly at all scales." Science 295.5564 (2002): 2418-2421. https://www.science.org/doi/10.1126/science.1070821
10. Yagai, Shiki, Takashi Karatsu, and Akihide Kitamura. "Photocontrollable self-assembly." Chemistry–A European Journal 11.14 (2005): 4054-4063. https://doi.org/10.1002/chem.200401323
11. Li, Z. P., et al. "Fabrication of nanopore and nanoparticle arrays with high aspect ratio AAO masks." Nanotechnology 28.9 (2017): 095301. DOI 10.1088/1361-6528/aa585c
12. Kim, Kyungtae, Moonjung Kim, and Sung M. Cho. "Pulsed electrodeposition of palladium nanowire arrays using AAO template." Materials chemistry and physics 96.2-3 (2006): 278-282. https://doi.org/10.1016/j.matchemphys.2005.07.013
13. Mijangos, Carmen, Rebeca Hernández, and Jaime Martin. "A review on the progress of polymer nanostructures with mod-ulated morphologies and properties, using nanoporous AAO templates." Progress in Polymer Science 54 (2016): 148-182. https://doi.org/10.1016/j.progpolymsci.2015.10.003
14. Kim, Dong Sung, et al. "Replication of high-aspect-ratio nanopillar array for biomimetic gecko foot-hair prototype by UV nano embossing with anodic aluminum oxide mold." Microsystem Technologies 13 (2007): 601-606. https://doi.org/10.1007/s00542-006-0220-1
15. Lee, Jae-Hwang, Jonathan P. Singer, and Edwin L. Thomas. "Micro-/nanostructured mechanical metamaterials." Advanced materials 24.36 (2012): 4782-4810. https://doi.org/10.1002/adma.201201644
16. Lee, Jae-Hwang, et al. "25th anniversary article: ordered polymer structures for the engineering of photons and phonons." Advanced Materials 26.4 (2014): 532-569. https://doi.org/10.1002/adma.201303456
17. Yang, Mingyu, et al. "Additive manufacturing of high aspect-ratio structures with self-focusing photopolymerization." Light: Advanced Manufacturing 3.3 (2022): 542-571. 10.37188/lam.2022.032
18. Kim, Seok, et al. "Microstructured surfaces for reducing chances of fomite transmission via virus-containing respiratory droplets." ACS nano 15.9 (2021): 14049-14060. https://doi.org/10.1021/acsnano.1c01636

19. Choi, Su Hyun, et al. "Tulip-shaped pattern imprinting for omni-phobic surfaces using partially cured photopolymer." Applied Sciences 11.4 (2021): 1747. https://doi.org/10.3390/app11041747
20. Shin, Seungwoo, et al. "Micro-replication platform for studying the structural effect of seed surfaces on wetting properties." Scientific Reports 12.1 (2022): 5607. https://doi.org/10.1038/s41598-022-09634-7
21. Kim, Woo Young, et al. "Quasi-seamless stitching for large-area micropatterned surfaces enabled by Fourier spectral analysis of moiré patterns." Nature Communications 14.1 (2023): 2202. https://doi.org/10.1038/s41467-023-37828-8
22. Chuang, Cheng-Hsin, et al. "Antireflective polymer films via roll to roll UV nanoimprint lithography using an AAO mold." Microsystem Technologies 24 (2018): 389-395. https://doi.org/10.1007/s00542-017-3299-7
23. Jeong, Yeonho, et al. "Fabrication of nano-micro hybrid structures by replication and surface treatment of nanowires." Crystals 7.7 (2017): 215. https://doi.org/10.3390/cryst7070215
24. Jeong, Yeonho, et al. "Multiscale structures aggregated by imprinted nanofibers for functional surfaces." JoVE (Journal of Visualized Experiments) 139 (2018): e58356. doi: 10.3791/58356
25. Kim, Youn-Su, et al. "Nanoimprint lithography patterns with a vertically aligned nanoscale tubular carbon structure." Nan-otechnology 19.36 (2008): 365305. DOI 10.1088/0957-4484/19/36/365305
26. Suehiro, Junya, et al. "Dielectrophoretic fabrication and characterization of a ZnO nanowire-based UV photosensor." Nano-technology 17.10 (2006): 2567. DOI 10.1088/0957-4484/17/10/021
27. Kim, Seonjun, et al. "Effect of surface pattern morphology on inducing superhydrophobicity." Applied Surface Science 513 (2020): 145847. https://doi.org/10.1016/j.apsusc.2020.145847
28. Kess, Robert S., et al. "Effect of surface treatments on the wettability of vinyl polysiloxane impression materials." The Journal of prosthetic dentistry 84.1 (2000): 98-102. https://doi.org/10.1067/mpr.2000.106720
29. Śmielak, Beata, et al. "Effect of zirconia surface treatment on its wettability by liquid ceramics." The Journal of Prosthetic Dentistry 122.4 (2019): 410-e1. https://doi.org/10.1016/j.prosdent.2019.06.021
30. Ahmed, Afaque, et al. "Development of surface treated nanosilica for wettability alteration and interfacial tension reduction." Journal of Dispersion Science and Technology 39.10 (2018): 1469-1475. https://doi.org/10.1080/01932691.2017.1417133
31. Ma, Kun, et al. "Wettability control and patterning of PDMS using UV–ozone and water immersion." Journal of colloid and interface science 363.1 (2011): 371-378. https://doi.org/10.1016/j.jcis.2011.07.036
32. Kuang, Ping, et al. "Improved surface wettability of polyurethane films by ultraviolet ozone treatment." Journal of Applied Polymer Science 118.5 (2010): 3024-3033. https://doi.org/10.1002/app.32712
33. Hamdi, Marouen, and Johannes A. Poulis. "Effect of UV/ozone treatment on the wettability and adhesion of polymeric sys-tems." The Journal of Adhesion 97.7 (2021): 651-671. https://doi.org/10.1080/00218464.2019.1693372
34. Kuang, Ping, Kristen Constant, and M. Aliofkhazraei. "Increased wettability and surface free energy of polyurethane by ultraviolet ozone treatment." Wetting and wettability (2015). http://dx.doi.org/10.5772/60798
35. Shin, Seunghang, Seok Kim, and Young Tae Cho. "Tunable Reverse Offset Printing with a Stretchable Blanket for Fabricating Flexible Printed Electronics." Advanced Engineering Materials 23.7 (2021): 2001537. https://doi.org/10.1002/adem.202001537
36. Cho, Woong, et al. "Surface modification effect of wettability on the performance of PDMS-based valveless micropump." Key Engineering Materials 326 (2006): 297-300. https://doi.org/10.4028/www.scientific.net/KEM.326-328.297
37. Stark, Alyssa Y., et al. "Surface wettability plays a significant role in gecko adhesion underwater." Proceedings of the National Academy of Sciences 110.16 (2013): 6340-6345. https://doi.org/10.1073/pnas.1219317110
38. Liu, D.; Wang, S.; Wu, T.; Li, Y. A Robust Superhydrophobic Polyurethane Sponge Loaded with Multi-Walled Carbon Nanotubes for Efficient and Selective Oil-Water Separation. Nanomaterials 2021, 11, 3344. https://doi.org/10.3390/nano11123344
39. Kim, Do Hyeog, et al. "Shape-deformed mushroom-like reentrant structures for robust liquid-repellent surfaces." ACS Applied Materials & Interfaces 13.28 (2021): 33618-33626. https://doi.org/10.1021/acsami.1c06286